RSC Advances

This is an *Accepted Manuscript*, which has been through the Royal Society of Chemistry peer review process and has been accepted for publication.

Accepted Manuscripts are published online shortly after acceptance, before technical editing, formatting and proof reading. Using this free service, authors can make their results available to the community, in citable form, before we publish the edited article. This *Accepted Manuscript* will be replaced by the edited, formatted and paginated article as soon as this is available.

You can find more information about *Accepted Manuscripts* in the Information for Authors.

Please note that technical editing may introduce minor changes to the text and/or graphics, which may alter content. The journal's standard Terms & Conditions and the Ethical guidelines still apply. In no event shall the Royal Society of Chemistry be held responsible for any errors or omissions in this *Accepted Manuscript* or any consequences arising from the use of any information it contains.

ROYAL SOCIETY OF CHEMISTRY

www.rsc.org/advances

Please do not adjust margins

Journal Name

ARTICLE

Oscillatory behaviour of the surface reduction process of multilayer graphene oxide at room temperature

Received 00th January 20xx,
Accepted 00th January 20xx

DOI: 10.1039/x0xx00000x

www.rsc.org/

D. N. Voylov[a]*, I. N. Ivanov[b,a]*, V. I. Bykov[c], S. B. Tsybenova[d], I. A. Merkulov[b], S. A. Kurochkin[e], A. P. Holt[a], A. M. Kisliuk[b], and A. P. Sokolov[a,b]

We report the observation of oscillatory redox reactions on the surface of multilayer graphene oxide (GO) films at room temperature. The redox reactions exhibited dampened oscillatory behavior with a period of about 5 days and found to be dependent on the time elapsed from film deposition. The kinetic behavior observed for the oxidation-reduction reactions and the metastability of the surface functional groups are adequately described by two models involving GO reactions and reactant diffusion.

1 Introduction

The dynamic research in the field of 2D materials, including graphene oxide (GO), has enabled the design of complex and novel device architectures based on their unique electrical, optical, and mechanical properties [1–7]. The relative low cost of production, tunability of surface chemistry [8], and the dispersibility in various solvents make GO an attractive candidate for multifunctional system design [9–17]. However, S. Kim *et al*. [18] showed that the chemical composition of single flake of multilayer GO is metastable on the time scale of one month at room temperature. The observed changes in chemical composition were attributed to a reduction process controlled by the in-plane diffusion of functional groups [18,19] which progresses through radical reactions [20–22]. Furthermore, it was reported that chemical modifications of GO are not stable and that they can change due to intramolecular reactions which inhibits the ability to create stable suspensions of GO [23,24].

There are several favorable conditions for autocatalytic and oscillatory chemical reactions[25] such as heterogeneity in the spatial distribution of chemical functionalities[26] , the differences in the reactant diffusion rates, media in-plane and out-of-plane directions[18,19,27–31], and enhanced reactivity at the edges of GO [32].

In this article, we report the observation of oscillatory redox reactions pertaining to the oxygen-containing functional groups on the surface of a multi-layered GO film under vacuum at room temperature, which was determined to occur for approximately 10 days. Additionally, we demonstrate that the oscillatory redox reactions and metastability can be well explained by two models related to the interplay between the slow diffusion of chemically bonded oxygen and hydrogen below the surfaces of the GO layers and the fast radical reactions occurring along the edges of the GO layers.

2 Experimental part

4.1 Synthesis of GO

Multilayered GO was synthesized using a modified Hummer's method [31]. The GO films were prepared from a centrifuged GO water solution by consecutively drop casting on a Teflon film to avoid adhesion. Before casting the films, the Teflon supports were cleaned by polar (tetrahydrofuran, THF) and non-polar (hexane) solvents in ultrasound bath.

4.2 X-ray photoelectron spectroscopy

X-ray photoelectron spectroscopy (XPS) was performed using ESCA with Phoibos-150 analyzer (SPECS, Germany). A non-monochromatized MgKα X-ray source was used ($h\nu$ = 1253.6 eV), that penetrates approximately 40 Å into the film. All the XPS signals were recorded with a pass energy equal to 30 eV. The pressure in the sample chamber did not exceed 8×10^{-10} Torr and the scanning conditions for all measurements were as the following: 100 ms/step, 0.1-0.05 eV/step, and 30 sweeps. We should note that samples were stored in the XPS vacuum chamber for the duration of the experiment and that the typical thickness of the GO films for XPS measurements were approx. 1 micron which is equivalent to several hundred single flakes of multi-layer GO.

The analysis of the XPS data were performed with CasaXPS 2.3.16Dev.52 software using the Marquardt's iteration method. For our data, the Tougaard background type was used and the fitting was done using the function defined as 20%

[a] University of Tennessee, Knoxville, TN, USA 37916-1600.
[b] Oak Ridge National Laboratory, Oak Ridge, TN, USA 37830.
[c] Emanuel Institute of Biochemical Physics RAS, Moscow, Russia, 119334.
[d] Moscow City Teacher Training University, Moscow, Russia, 129226.
[e] Institute of Problems of Chemical Physics RAS, Chernogolovka, Russia, 142432
* - Corresponding authors, Email address: dvoylov@utk.edu, ivanovin@ornl.gov.
Electronic Supplementary Information (ESI) available. See DOI: 10.1039/x0xx00000x

RSC Advances Accepted Manuscript

Lorentzian and 80% Gaussian (the same analysis method utilized in Ref.33). The spectra of the initial GO film revealed electrostatic charging. Since the same material was used to prepare all GO films it is reasonable to expect the same average value of binding energies for "C-C" electrons. We obtained this value (284.6 eV) based on experimental results of thermally reduced GO. Thus, the electrostatic charging shift was corrected for all spectra in CasaXPS using the calibration utility.

4.3 Scanning probe microscopy

Scanning probe microscopy (SPM) measurements were performed using a Scanning Probe Nanolaboratory Integra Aura (NT-MDT, Russia) and OmegaScope (AIST-NT, Novato, USA). Three types of tips were used: (1) standard silicon tips with a radius of curvature ~ 10 nm, (2) supersharp DLC tips with a radius of curvature ~ 1 nm for studying topology in a tapping mode (NanoSensor, USA), and (3) Scanning Kelvin Probe Microscopy (SKPM) measurements were performed under low vacuum (about 50 mbar) using standard tips covered by PtIr (radius of curvature ~ 20 nm) with a WF ~5.2 eV, which were previously calibrated by measurements of fresh cleaved HOPG surface with a stable value of WF = 4.6 eV. For scanning Kelvin probe microscopy measurements, an AC voltage with an amplitude of $\boldsymbol{V}_{AC}$ = 0.2 V at a frequency of $\boldsymbol{f}$ = 154.657 kHz was applied to a probe. It should be noted that during all tapping-mode and SKPM measurements the amplitude of tip deviation was ~ 4 nm.

For SPM measurements, the initial samples of GO were prepared by the following method: a water solution with a volume of 10 µl was drop-casted onto a substrate and was subsequently absorbed by filter paper (without touching the surface) after 60 seconds. For positive GO sheet identification, a fresh flake of HOPG was attached to a pyroceram glass with bi-adhesive tape and placed on the scanner with a maximum scanning range of 100 microns. A number of SPM measurements detected the displacement of the substrate due to the reversible deformation of the bi-adhesive tape. As a result, the sample was left untouched for 24 hours and then was re-scanned. This procedure was repeated until the displacement was within acceptable bounds (no more than 2.0 nm/1.5 min).

4.4 Raman spectroscopy

Raman measurements were performed in a backscattering geometry using a Jobin Yvon T64000 triple monochromator spectrometer together with a Coherent Verdi II solid-state laser (wavelength of 532 nm with a power of 0.5 mW).

3 Results

The initial flakes of GO were characterized using scanning probe microscopy (Figure 1), infrared (IR) and Raman spectroscopy (Figure 2). The contact potential difference (Figure 1b) of the GO measured by SKPM with a previously calibrated tip (work function (WF) of the tip ≈ 5.2 eV) is proportional to the difference between WF of the tip material and the sample [34]. From these measurements, the WF of GO was estimated to be ~4.85 eV. This value is in good agreement with literature and implies that synthesized GO typically contains oxygen in the form of epoxy and hydroxyl groups [27].

IR absorbance spectrum is shown in Figure 2a. The regions with high absorbance coefficients were assigned to vibration modes of C-O and hydroxyl containing modes (C-OH, COOH, H_2O) in the ranges of 800 – 1370 cm^{-1} and 3000-3700 cm^{-1} respectively (as it was made, for example in the Ref. 6). The absorbance at 1580 cm^{-1} was attributed to in-plane stretching of sp^2-hybridized carbons (C=C) with a possible contribution of ketone and/or carbonyl group (C=O) vibrations (which also has absorbance around 1735 cm^{-1}). The shoulder at 2850 cm^{-1} was assigned to C-H vibration modes of alkyl type chains. Results from Raman spectroscopy are shown in Figure 2b and contains the typical spectra for GO, *e.g.*, the G (1354 cm^{-1}) and D (1605 cm^{-1}) bands.

The evolution of chemical functionalities was studied using XPS. The analysis and deconvolution of XPS data was based on known chemical shifts of electron binding energy of atoms in compounds and the integral intensity of peaks which is directly proportional to concentration of the atoms [35,36]. Typically, the core-level C1s spectra are fit by 2-5 functions depending on strength or visibility of components [35]. The XPS spectra in the C1s region (from 281 to 292 eV of binding energy) is shown in Figure 3 a,b where the change in the integrated areas, or concentration of atoms, of the deconvoluted peaks as a function of time is apparent (see the SI for more details).

The first maximum on the spectra at 284.6 eV (Figure 3b) was attributed to the electrons from carbon atoms in sp^2 (Csp^2), sp^3 (Csp^3) hybridization [37] and to the chemically bonded carbon with hydrogen (C-H) (further referred to as C-C)[38]. The contributions from defects, carbon atoms in the structure of 5–8–5 defects, and Stone–Wales defects [39,40] are expected to have binding energy slightly higher than that of Csp^2 (about 0.5 eV, full width at half maximum (FWHM) of about 2 eV) [41]. Therefore, C-H, Csp^3 and "defects" contribute to the broadening of C-C peak, which usually has FWHM of about 1 eV for aromatic layers in Csp^2 hybridization. The high-energy peaks of the spectrum were attributed to the hydroxyl (286.2 eV), epoxy/ether (286.8 eV), carbonyl (288.1 eV) and carboxyl (289.3 eV) functional groups [37] (Figure 3b) (for more details related to deconvolution procedure, see SI). In the literature, it is widely accepted that the electronic energies of carbon bonded to hydroxyl or epoxy groups have very similar values which prevents the deconvolution of their contributions to the C1s spectra from XPS. It is important to note that oscillatory behavior does not depend on how many components were used during deconvolution procedure. In fact, all the evidence supporting the oscillatory behavior presented in this work, as it will be shown, stems from the analysis of the C-C component. The specific reason to use five functions was due to the shift of the maximum at around 286 eV to a low energy during the experiment (Figure 3b inset) (for more details, see SI). This shift can only be explained by a relaxation process or a change

RSC Advances Accepted Manuscript

This journal is © The Royal Society of Chemistry 20xx

in contributions to the spectra from different functionalities. Our dielectric measurements did not reveal any process with such a long relaxation time (~10^4 min). Therefore, we believe the shift is caused by changes of epoxy/hydroxyl functional group concentration ratio which correlates with the degree of GO reduction (C-C concentration) as shown in Figure S2 and S3.

Unfortunately, IR and Raman spectroscopy do not reveal any essential difference between the initial GO and the GO after eleven days of measurements. We believe that this is caused by difference of sampling depth (or escape depth of photoelectrons) and measurement conditions. The XPS technique provides information concerning the chemical composition of surface with a typical sampling depth of about 4 nm (for this material). By taking into account X-ray beam diameter (50 μm) it is easy to estimate that the XPS allows to analyze a chemical composition of about 10^{11} atoms or 10^{-13} mole of substance on a surface. However, IR and Raman spectroscopy integrate their signal from a volume several orders of magnitudes larger and have a much lower sensitivity to the surface. In addition, it should be noted, that the XPS measurements are performed in a high vacuum while IR and Raman spectroscopy work under ambient conditions. This difference may be crucial if water molecules adsorbed on the surface of the GO and participate in chemical reactions or the reduction process.

4 Discussion

The time-dependence for the concentration of the functional groups are shown on the Figures 4a-e. It becomes apparent that the concentration of C-C (Figure 4a), hydroxyl (Figure 4b) and epoxy/ether (Figure 4c) groups changes significantly as a function of time. However, the concentrations of carbonyl (Figure 4d) and carboxyl (Figure 4e) functional groups undergo rather small changes. The changes in the water content is shown in Figure 4f. These results indicate that there are complex chemical reactions are occurring on the surface of GO under vacuum at room temperature over the course of eleven days.

S. Kim proposed that the reduction of GO occurs through the reactions between chemically bonded hydrogen (C-H) and hydroxyl groups (C-OH) on the surface of GO [18].

$$\{C\text{-}H\} + \{C\text{-}OH\} \rightarrow \{C=C\} + H_2O\uparrow \quad (1)$$

The loss of hydroxyl group is compensated by a reaction between epoxy groups (C-O-C) and C-H:

$$\{C\text{-}H\} + \{C\text{-}O\text{-}C\} \rightarrow \{C=C\} + \{C\text{-}OH\} \quad (2)$$

However, these reactions alone cannot explain the observed oscillatory behavior. In addition to the reactions (1) and (2), we considered the diffusion of functionalities in both the in-plane and out-of-plane directions. Also, we suggest another model based on facile reactions along the edges of GO layer between defect sites.

3.1 Diffusivity model

The diffusivity model, based on the reactions (1) and (2) considers the diffusion of the oxygen and hydrogen containing functional groups throughout the multilayered GO. The diffusive processes follow from a simple analysis of the kinetic behavior (Figure 4). This behavior may be conditionally divided into four regions corresponding to the time intervals with the prevalent chemical processes. The **first region** (0-5,000 min) reveals the growth in the concentration of C-C bonds (Figure 4a) which corresponds to intensive reduction. It is also accompanied by a decrease in the FWHM (Figure 4g) and charging shift (Figure 4g). The charging shift reflects the resistivity of the material and therefore the size of π-conjugated domains which percolate throughout the volume of the film. The continued growth in the concentration of C-C bonds during the times from 5,000 to 7,500 min was allocated into **region II** due to a simultaneous change in the trend of the charging shift and FWHM of the C-C peak (Figures 4a and 4g). The broadening of C-C maximum accompanied by an increase of the charging shift (Figure 4h) can be explained only by a considerable growth in the concentration of C-H, Csp^3 or "defects" sites. Based on general considerations, literature data, and Raman spectra which have not revealed any difference for the GO film before and after XPS measurements we cannot conclude any reasons why the concentration of "defects" might spontaneously increase at room temperature and under vacuum. The SPM results (Figure 1) also showed that pristine GO does not possess indented edges or holes which are typical for high defective sheets [42]. The **third stage** (7,500-12,000 min) (Figure 4a) shows the re-oxidation of GO. Recently, M. Acik *et al.* [21] reported an increase in the degree of oxidation of GO at a temperature of 200°C. Also, we previously reported the observation of re-oxidation of microwave exfoliated graphite oxide in storage under an ambient air atmosphere at room temperature [42]. The **fourth stage** (12,000-16,000 min) is dominated by the reduction process.

The material balance analysis suggests that the re-oxidation of the GO surface under vacuum occurred due to the diffusion of oxygen functionalities. The possible ways for oxygen and its functionalities to diffuse are through the defects and edges of graphene oxide sheet because of the large steric factor for motion through the structure. The hydrogen atom does not have steric constraints for the inter- and intra- layers hopping in GO sheets because of its small size and sufficient space in GO structure [44]. The case of different diffusion paths for hydrogen and oxygen functional groups should lead to a different space localization on the surface. Also, in the case of carbon nanotubes it was shown that diffusing hydrogen is more probable to form pairs [45]. We believe that consumption of the initial hydrogen occurring during the reduction in the **stage I**, leads to a concentration gradient of hydrogen in a transverse direction which causes diffusion. Water molecules that are intercalated in the interlayer space may play an important role and act as the buffer for hydrogen and oxygen due to the reactions with

RSC Advances Accepted Manuscript

carbon radicals that are released during the reduction process. A detailed schematic representation of this model is illustrated in Figure 5.

Based on the kinetics of the "C-C" bond concentration and the fact that hydrogen should diffuse at least through one interlayer distance to maintain the observed contribution in the XPS spectra, we estimate that the higher limit of diffusion coefficient has a value order of 10^{-10} cm^2/s. This value is only one order of magnitude lower than the in-plane diffusion coefficient of physio-adsorbed hydrogen in graphite [46]. In order to evaluate this model, we propose that diffusion is facilitated by the reactions of functionalities from the inner layers with carbon radicals. The oscillatory-like behavior is known to take place in the systems with a spatially separated localization of reagents [30,25]. The diffusing hydrogen through GO may form pairs, as was previously reported in carbon nanotubes [45]. The radical reactions are believed to define the degree of oxidation in the volume and on the surface of GO [21].

It is probable that the same radical reactions can facilitate the spatial separation of functional groups [26]. The existence of the carbon radical $\{C^{\bullet}\}$ is reasonable based on a literature [21, 47, 48] and when we take into account the possible formations of the transitional state complex {H-C-OH} in reaction (1) [49]. The carbon radical is expected to have a long enough life time to react with water molecules or participate in other reactions, leading to the transfer of functionalities from the bottom layers to the surface of GO. Likewise, the carbon radical can move in the plane of the GO surface as well as migrate along the structure of the π-system [50].

By accounting for the diffusion of functional groups and the existence of carbon radicals, the simplest modification of reactions (1) and (2) are:

$$\{COH\} + \{CH\} \longrightarrow \{C\text{-}C^{\bullet}\} + H_2O + e^- \quad (3)$$

$$\{COC\} + \{CH\} \longrightarrow \{C\text{-}C^{\bullet}\} + \{COH\} + e^- \quad (4)$$

$$\{C\text{-}C^{\bullet}\} + e^- \longrightarrow \{C=C\} \quad (5)$$

The presented reactions (3-5) along with the consideration for the diffusion of reactants lead to a system of non-linear differential equations. Our analysis demonstrates that oscillatory relaxations are probable for certain parameter values with small deviations and very likely for large deviations from the steady state (for more details, see SI). The deviations from a steady-state may be caused by the evaporation of water from the GO surface.

3.2 Reactive edges and defects model

We employed the following set of reactions for the examination of the reactive edges and defects, as model:

$$(O_2) + 2\{Z\} \rightleftarrows 2\{ZO\}, \quad (6)$$

$$(H_2) + 2\{Z\} \rightleftarrows 2\{ZH\}, \quad (7)$$

$$\{ZO\} + \{ZH\} \rightleftarrows \{Z\} + \{ZOH\}, \quad (8)$$

$$\{ZOH\} + \{ZH\} \longrightarrow 2\{Z\} + (H_2O), \quad (9)$$

$$(H_2O) + \{Z\} \rightleftarrows ZH_2O, \quad (10)$$

$$(H_2) + \{Z\} \rightleftarrows \{ZH_2\}, \quad (11)$$

$$\{ZH_2\} + \{ZO\} \longrightarrow 2\{Z\} + (H_2O), \quad (12)$$

$$2\{Z\} \rightleftarrows \{C=C\}, \quad (13)$$

Where *Z* – is active site on the GO sheet (i.e., carbon radical). The reactions (6), (7), (10-12) may be realized on the edges of graphene plane or defects located in the center of a GO sheet. The diffusion of hydrogen atoms in the plane of the GO surface has been reported in the literature [51,52]. The hydrogen atom does not have steric constraints for the inter- and intra- layer hopping in the GO layers because of its small size and the adequate space in GO structure [44]. The molecular species of oxygen released during the reduction of GO was reported by R. Larciprete and co-authors [20]. R.Y.N. Gengler *et al*. recently reported the interaction between water and graphene oxide on the timescale of picoseconds [53]. The remaining components are typical for GO chemical reactions [24].

The reactions (6), (11), (12) represent the simplest catalytic trigger, i.e. a system with three stationary states. The reaction (10) alone could lead to continuous oscillations. The remaining reactions lead to a non-stationary condition and dampened oscillations. The observed behavior is typical for a heterogeneous catalytic reaction where the fluctuation of reaction rates on the catalyst surface can induce a transient behavior in the catalyst volume [25], which is important since the catalytic reactions in GO are known to occur on the edges [54]. The deactivation of graphene active centers through reaction (13) is irreversible, and leads to dampened oscillations within the system.

The analysis of experimental results by this model is shown on the Figure 6. Figure 6a shows a single measurement fit using the "reactive edges" model. A comparison of experimental results beginning after the initial deposition of GO to those obtained by S. Kim and co-authors in Ref. [18] is shown in the Figure 6b. The data was fit using equation:

$$C_{C\text{-}C,\%}(t) = C_1 - C_2 e^{-\frac{t}{k_1}} + C_3 e^{-\frac{t}{k_2}} \sin(k_3 t - k_4)$$

This is one of possible analytical solutions of the system of differential equations, which satisfies the reactions in this model.

The results of additional measurements of nine different samples are presented on the Figure 6c along with previously reported results in Ref. [18]. We found a correlation between the functional group concentrations and the time elapsed after the water evaporation. We normalized the data on time elapsed from the deposition procedure (i.e., water evaporation) introducing a time parameter, t_d, which accounts for the time from when the initial GO deposition occurred. By taking into

RSC Advances Accepted Manuscript

This journal is © The Royal Society of Chemistry 20xx

account that the samples were stored in a dark place (to avoid photo reduction) and at room temperature after the initial GO deposition, we conclude that the evaporation of water plays a crucial role in these effects.

5 Conclusions

We observed the oscillation in the concentrations of oxygen-containing functionalities on the surface of GO on the timescale of approximately 11 days. Our experiments revealed that the amplitude of oscillations depends on time elapsed from the deposition of GO. We proposed two models based on (1) the chemical reactions along the edges of GO and defects, and (2) the diffusion phenomena of functionalities.

Our analyses demonstrate that both models well describe the experimental results and may be complementary processes. The mechanism based on the diffusion phenomena is likely to stem from the successive accumulation and consumption of chemically bonded oxygen (mainly hydroxyl and epoxy groups) and hydrogen species on the GO surface which lead to radical reactions. The diffusion of oxygen-containing functionalities may have higher steric hindrance in comparison with those based on hydrogen diffusion.

The rate constant of GO reduction at room temperature obtained by S. Kim and co-authors [18] (relaxation time was estimated to be equal to ~35 days) are probably applicable to the processes occurring on the timescale of > 30 days. Many functionalities with unresolvable peak positions from XPS measurements limited the estimation of reaction rate constants. There are further experiments are required to fully understand the complexity of these reactions.

Acknowledgements

This work was supported by the U.S. Department of Energy, Office of Science, Basic Energy Sciences, Materials Sciences and Engineering Division. A portion of this research was conducted at the Center for Nanophase Materials Sciences ORNL, which is a DOE Office of Science User Facility.
D.N.V. thanks Prof. Gustavo A. Carri, Dr. Eric Olsen, Prof. Bobby G. Sumpter for the helpful discussions.
This manuscript is dedicated to the memory of late Dr. Igor A. Merkulov, who passed away on July 4, 2014, while working on revisions to this manuscript.

Notes and references

Corresponding authors: Dmitry Voylov: dvoylov@utk.edu; Ilia Ivanov: ivanovin@ornl.gov,
[a] Department of Chemistry, University of Tennessee, Knoxville, TN, USA 37916-1600,
[b] Oak Ridge National Laboratory, Oak Ridge, TN, USA 37830
[c] Emanuel Institute of Biochemical Physics RAS, Moscow, Russia, 119334
[d] Moscow City Teacher Training University, Moscow, Russia, 129226
[e] Institute of Problems of Chemical Physics RAS, Chernogolovka, Russia, 142432

† Footnotes should appear here. These might include comments relevant to but not central to the matter under discussion, limited experimental and spectral data, and crystallographic data.
Electronic Supplementary Information (ESI) available: [details of any supplementary information available should be included here]. See DOI: 10.1039/b000000x/

This manuscript has been authored by UT-Battelle, LLC under Contract No. DE-AC05-00OR22725 with the U.S. Department of Energy. The United States Government retains and the publisher, by accepting the article for publication, acknowledges that the United States Government retains a non-exclusive, paid-up, irrevocable, world-wide license to publish or reproduce the published form of this manuscript, or allow others to do so, for United States Government purposes. The Department of Energy will provide public access to these results of federally sponsored research in accordance with the DOE Public Access Plan (http://energy.gov/downloads/doe-public-access-plan).

Author contributions

D.N.V. conceived the idea, synthesized materials, performed the XPS and SPM experiments and processed the data. I.N.I., A.M.K., A.P.H. performed the Raman and IR spectroscopy experiments and processed the data. V.I.B., S.B.T. developed and analyzed “reactive edges and defects model”. I.A.M., I.N.I, S.A.K., D.N.V., A.P.S. developed and analyzed “diffusivity model”. A.P.S, D.N.V., I.N.I., A.P.H., S.A.K wrote the manuscript. All authors contributed to the review of the manuscript and the discussion of the results.

Additional information

The authors declare no competing financial interests.

References

1 D. Li and R. B. Kaner, *Science,* 2008, **320**, 1170.
2 A. K. Geim and K. S. Novoselov, *Nat. Mater.,* 2007, **6**, 183.
3 A. K. Geim, *Science,* 2009, **324**, 1530.
4 Y. Zhu, S. Murali, W. Cai, X. Li, J. W. Suk, J. R. Potts and R. S. Ruoff, *Adv. Mater.,* 2010, **22**, 3906.
5 S. Park and R. S. Ruoff, *Nat. Nanotechnol.,* 2009, **4**, 217.
6 D. Chen, L. Tang and J. Li, *Chem. Soc. Rev.,* 2010, **39**, 3157.
7 H. Jiang, *Small,* 2011, **7**, 2413.
8 D. R. Dreyer, S. Park, C. W. Bielawski and R. S. Ruoff, *Chem. Soc. Rev.,* 2010, **39**, 228.
9 D. Chen, H. Feng and J. Li, *Chem. Rev.,* 2012, **112**, 6027.
10 T. Y. Kim, H. W. Lee, M. Stoller, D. R. Dreyer, C. W. Bielawski, R. S. Ruoff and K. S. Suh, *ACS Nano,* 2011, **5**, 436.
11 J. Zou and F. Kim, *Nat. Commun.,* 2014, **5**, 5254.
12 C. Berger , Z. Song, T. Li, X. Li, A. Y. Ogbazghi, R. Feng, Z. Dai, A. N. Marchenkov, E. H. Conrad, P. N. First and W. A. de Heer, *J. Phys. Chem. B,* 2004, **108**, 19912.
13 S. Stankovich, D. A. Dikin, G. H. B. Dommett, K. M. Kohlhaas, E. J. Zimney, E. A. Stach, R. D. Piner, S. T. Nguyen and R. S. Ruoff, *Nature,* 2006, **442**, 282.
14 K. S. Kim, Y. Zhao, H. Jang, S. Y. Lee, J. M. Kim, K. S. Kim, J.-H. Ahn, P. Kim, J.-Y. Choi and B. H. Hong, *Nature,* 2009, **457**, 706.

RSC Advances Accepted Manuscript

15 F. Bonaccorso, Z. Sun, T. Hasan and A. C. Ferrari, *Nat. Photonics,* 2010, **4**, 611.
16 D. A. Dikin, S. Stankovich, E. J. Zimney, R. D. Piner, G. H. B. Dommett, G. Evmenenko, S. T. Nguyen and R. S. Ruoff, *Nature,* 2007, **448**, 457.
17 K. Zhang, *Appl. Surf. Sci.,* 2012, **258**, 7327.
18 S. Kim, S. Zhou, Y. Hu, M. Acik, Y. J. Chabal, C. Berger, W. de Heer, A. Bongiorno and E. Riedo, *Nat. Mater.,* 2012, **11**, 544.
19 S. Zhou and A. Bongiorno, *Sci. Rep.,* 2013, **3**, 2484.
20 R. Larciprete, S. Fabris, T. Sun, P. Lacovig, A. Baraldi and S. Lizzit, *J. Am. Chem. Soc.,* 2011, **133**, 17315.
21 M. Acik, G. Lee, C. Mattevi, A. Pirkle, R. M. Wallace, M. Chhowalla, K. Cho and Y. Chabal, *J. Phys. Chem. C,* 2011, **115**, 19761.
22 F. Barroso-Bujans, Á. Alegría and J. Colmenero, *J. Phys. Chem. C,* 2010, **114**, 21645.
23 H. He, T. Riedl, A. Lerf and J. Klinowski, *J. Phys. Chem.* 1996, **100**, 19954.
24 D. R. Dreyer, S. Park, C. W. Bielawski and R. S. Ruoff, *Chem. Soc. Rev.,* 2010, **39**, 228.
25 G. S. Yablonskii, V. I. Bykov, V. I. Elokhin and A. N. Gorban, *Kinetic Models of Catalytic Reactions,* Elsevier, 1991.
26 M. P. McDonald, A. Eltom, F. Vietmeyer, J. Thapa, Y. V. Morozov, D. A. Sokolov, J. H. Hodak, K. Vinodgopal, P. V. Kamat and M. Kuno, *Nano Lett.* 2013, **13**, 5777.
27 P. V. Kumar, M. Bernardi and J. C. Grossman, *ACS Nano,* 2013, **7**, 1638.
28 D. W. Boukhvalov, M. I. Katsnelson and Y. W. Son, *Nano Lett.,* 2013, **13**, 3930.
29 R. K. Joshi, P. Carbone, F. C. Wang, V. G. Kravets, Y. Su, I. V. Grigorieva, H. A. Wu, A. K. Geim and R. R. Nair, *Science,* 2014, **343**, 752.
30 I. R. Epstein, *Nature,* 1995, **374**, 321.
31 D. N. Voylov, A. L. Agapov, A. P. Sokolov, Y. M. Shulga and A. A. Arbuzov, *Carbon N. Y.,* 2014, **69**, 563.
32 V. Schwartz, W. Fu, Y.-T. Tsai, H. M. Meyer III, A. J. Rondinone, J. Chen, Z. Wu, S. H. Overbury and C. Liang, *ChemSusChem,* 2013, **6**, 840.
33 T.Y. Leung, W.F. Man, P.K. Lim, W.C. Chan, F. Gaspari, S. Zukotynski, J. Non. Cryst. Solids, 1999, 254, 156.
34 N. Ashcroft, *Solid state physics*, Saunders college, 1976.
35 J. F. Moulder, *Handbook of X-ray Photoelectron Spectroscopy: A Reference Book of Standard Spectra for Identification and Interpretation of XPS Data*, Physical Electronics, 1995.
36 H. Hantsche, *Adv. Mater.,* 1993, **5**, 778.
37 K. Haubner, J. Murawski, P. Olk, L. M. Eng, C. Ziegler, B. Adolphi and E. Jaehne, *ChemPhysChem,* 2010, **11**, 2131.
38 A. Nikitin, L.-Å. Näslund, Z. Zhang and A. Nilsson, *Surf. Sci.,* 2008, **602**, 2575.
39 K. N. Kudin, B. Ozbas, H. C. Schniepp, R. K. Prud'homme, I. A. Aksay and R. Car, *Nano Lett.,* 2008, **8**, 36.
40 H. C. Schniepp, J.-L. Li, M. J. McAllister, H. Sai, M. Herrera-Alonso, D. H. Adamson, R. K. Prud'homme, R. Car, D. A. Saville and I. A. Aksay, *J. Phys. Chem. B,* 2006, **110**, 8535.
41 H. Estrade-Szwarckopf, *Carbon N. Y.,* 2004, **42**, 1713.
42 M. Cheng, R. Yang, L. Zhang, Z. Shi, W. Yang, D. Wang, G. Xie, D. Shi and G. Zhang, *Carbon N. Y.,* 2012, **50**, 2581.
43 Y. M. Shulga, S. A. Baskakov, E. I. Knerelman, G. I. Davidova, E. R. Badamshina, N. Yu. Shulga, E. A. Skryleva, A. L. Agapov, D. N. Voylov, A. P. Sokolov and V. M. Martynenko, *Rsc Adv.,* 2014, **4**, 587.
44 A. Buchsteiner, A. Lerf and J. Pieper, *J. Phys. Chem. B,* 2006, **110**, 22328.
45 Z. Zhang and K. Cho, *Phys. Rev. B,* 2007, **75**, 075420.
46 I. E. Gabis, *Semiconductors,* 1997, **31**, 110.
47 F. Beckert, A. M. Rostas, R. Thomann, S. Weber, E. Schleicher, C. Friedrich, and R. Mülhaupt, *Macromolecules* 2013, **46**, 5488
48 D. Voylov, T. Saito, B. Lokitz, D. Uhrig, Y. Wang, A. Agapov, A. Holt, V. Bocharova, A. Kisliuk, and A. P. Sokolov, *ACS Macro Lett.* 2016, **5**, 199
49 K. J. Laidler, *Theories of chemical reaction rates*, McGraw-Hill, 1969.
50 L. Yang, R. Zhang, B. Liu, J. Wang, S. Wang, M.-Y. Han and Z. Zhang, *Angew. Chem. Int. Ed. Engl.,* 2014, **53**, 10109.
51 L. Hornekær, E. Rauls, W. Xu, Ž. Šljivančanin, R. Otero, I. Stensgaard, E. Lægsgaard, B. Hammer and F. Besenbacher, *Phys. Rev. Lett.,* 2006, **97**, 186102.
52 S. Baouche, G. Gamborg, V. V. Petrunin, A. C. Luntz, A. Baurichter and L. Hornekær, *J. Chem. Phys.,* 2006, **125**, 084712.
53 R. Y. N. Gengler, D. S. Badali, D. Zhang, K. Dimos, K. Spyrou, D. Gournis and R. J. D. Miller, *Nat. Commun.,* 2013, **4**, 2560.
54 G. K. P. Dathar, Y.-T. Tsai, K. Gierszal, Y. Xu, C. Liang, A. J. Rondinone, S. H. Overbury and V. Schwartz, *ChemSusChem,* 2014, **7**, 483.

Figure captions:

Figure 1. (a) AFM results (tapping mode) of deposited on fresh cleaved mica GO flakes, (b) SKPM measurements results of GO deposited on fresh cleaved HOPG.

Figure 2. (a) IR and (b) Raman spectra of GO. There was no essential difference in spectra of initial GO and after 12 days of experiment.

Figure 3. Experimental data and fitting of X-ray photoelectron spectra in C1s electrons region: (a) The time evolution of the XPS shown as a surface plot. (b) The experimental data (open circles) with fitting curves (solid lines): C-C (black), hydroxyl groups (red), epoxy/ether groups (blue), carbonyl groups (green), carboxyl groups (magenta). Inset: The shift of the peak maximum at ~286.5 eV which was observed during all measurements.

Figure 4. The time evolution of concentration of C-C (a), C-OH and C-O-C (b), and C=O and COOH (c), carbonyl (d), carboxyl (e), and water (f) functional groups derived from the deconvolution of XPS spectra. (g) The full width at half maximum (FWHM) of the C-C functional group and (h) the charging shift.

Figure 5. A detailed schematic representation of the stages allocated from the time evolution of GO surface functionalities.

Figure 6. Dependence of C-C concentration on time. (a) Experimental results (red circles) and fitting using the "reactive edges" model (blue curve) of single measurement. (b) Comparison of experimental results started right after GO deposition (symbols), results obtained by S. Kim and co-authors in Ref. 18 (green stars), and the fitting based on the "reactive edges" model (red curve). (c) Comparison of all experimental data in the present work normalized on time elapsed from the deposition procedure (symbols), results obtained by S. Kim and co-authors in Ref. 18 (green stars), and the fitting based on the "reactive edges" model (red curve).

RSC Advances Accepted Manuscript

This journal is © The Royal Society of Chemistry 20xx

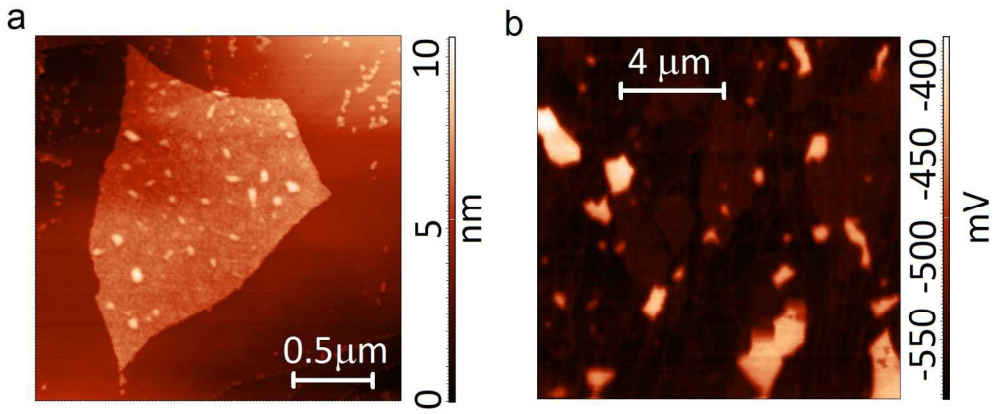

Figure 1. (a) AFM results (tapping mode) of deposited on fresh cleaved mica GO flakes, (b) SKPM measurements results of GO deposited on fresh cleaved HOPG.

478x201mm (96 x 96 DPI)

RSC Advances Accepted Manuscript

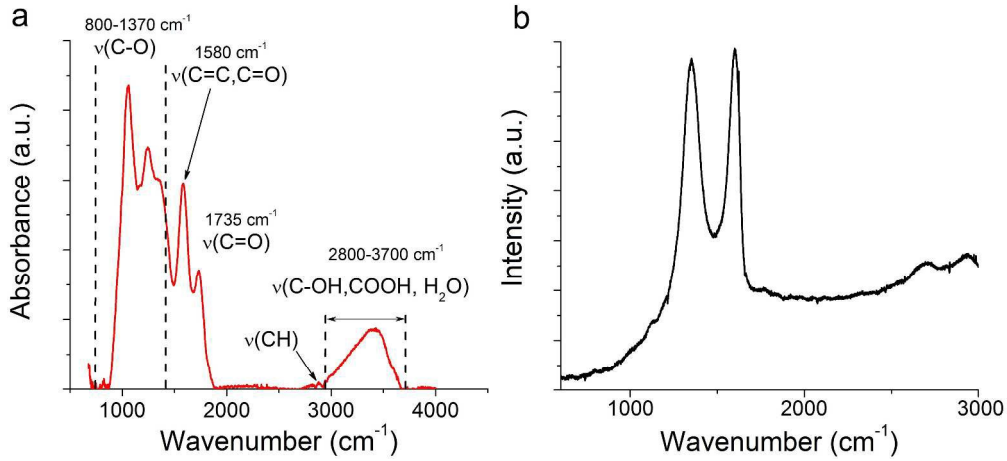

Figure 2. (a) IR and (b) Raman spectra of GO. There was no essential difference in spectra of initial GO and after 12 days of experiment.

422x191mm (300 x 300 DPI)

RSC Advances Accepted Manuscript

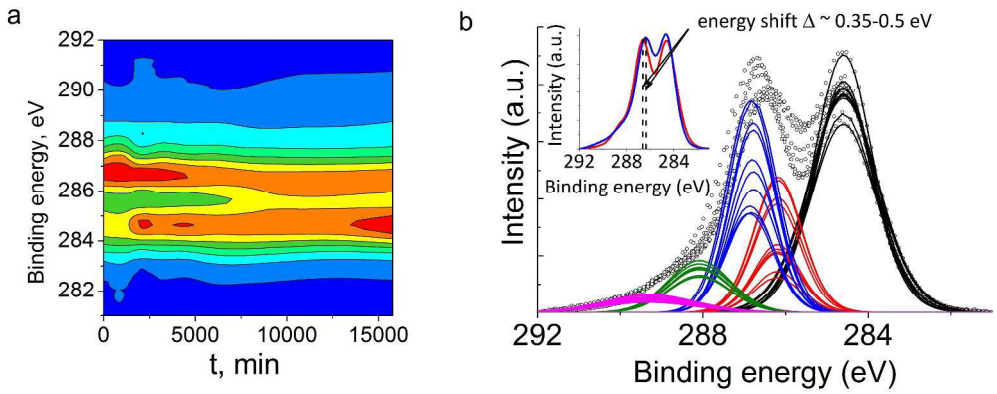

Figure 3. Experimental data and fitting of X-ray photoelectron spectra in C1s electrons region: (a) The time evolution of the XPS shown as a surface plot. (b) The experimental data (open circles) with fitting curves (solid lines): C-C (black), hydroxyl groups (red), epoxy/ether groups (blue), carbonyl groups (green), carboxyl groups (magenta). Inset: The shift of the peak maximum at ~286.5 eV which was observed during all measurements.

512x210mm (300 x 300 DPI)

RSC Advances Accepted Manuscript

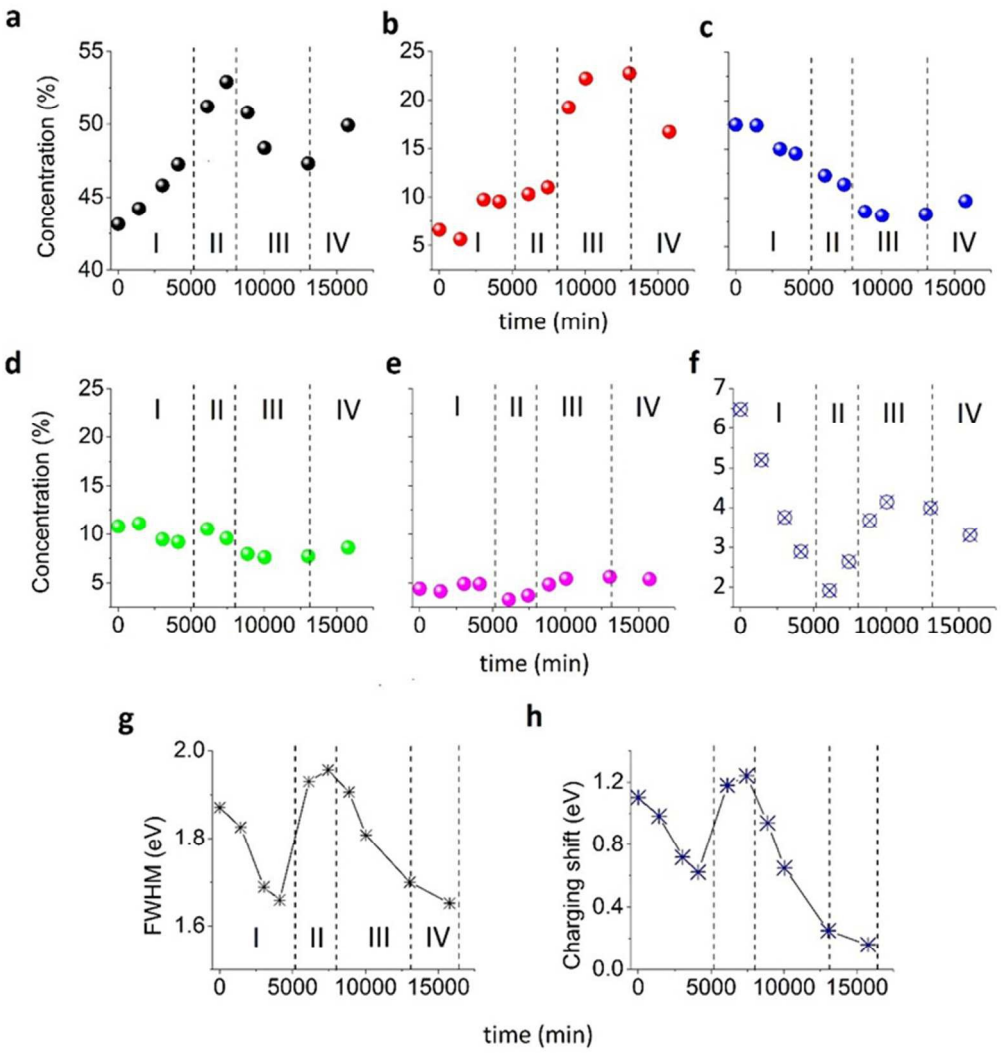

Figure 4. The time evolution of concentration of C-C (a), C-OH and C-O-C (b), and C=O and COOH (c), carbonyl (d), carboxyl (e), and water (f) functional groups derived from the deconvolution of XPS spectra. (g) The full width at half maximum (FWHM) of the C-C functional group and (h) the charging shift.

RSC Advances Accepted Manuscript

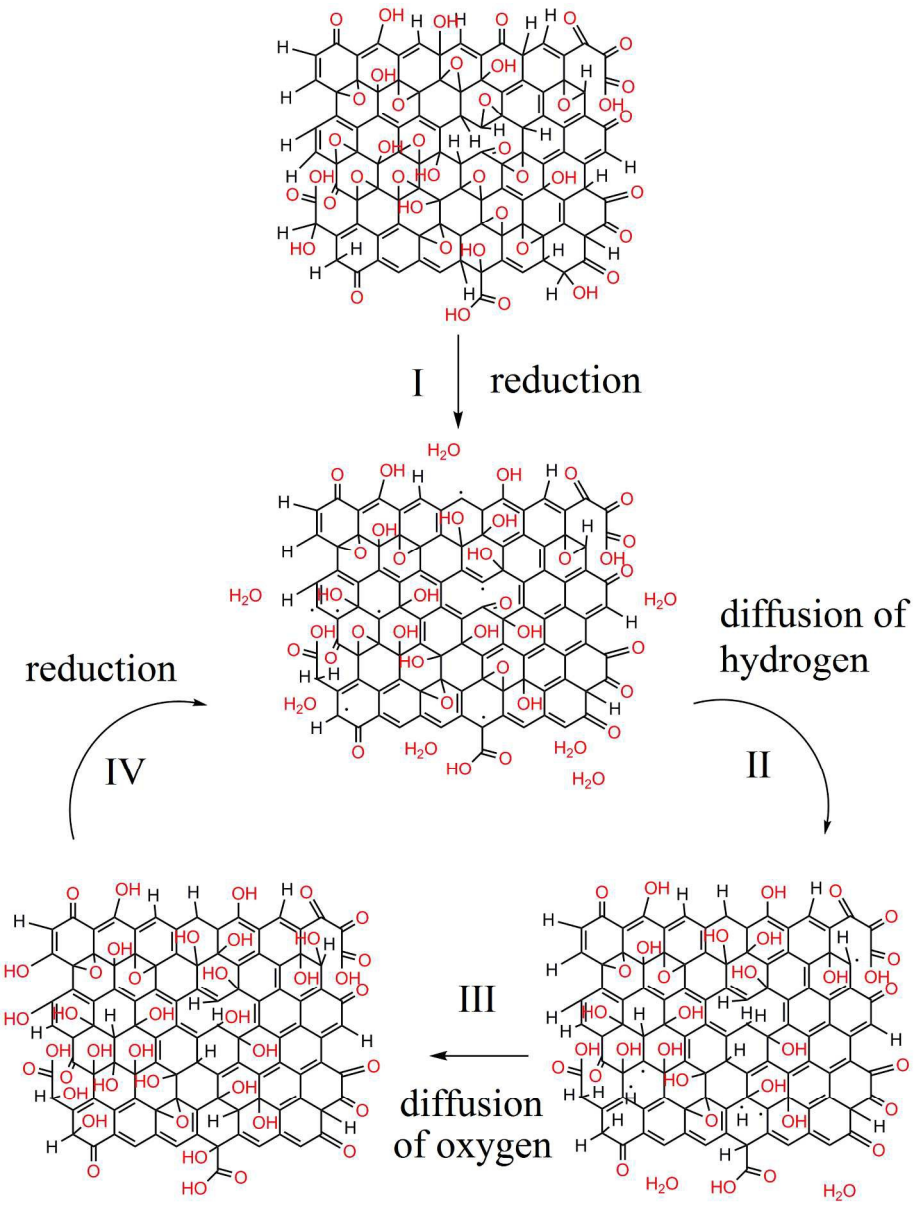

Figure 5. A detailed schematic representation of the stages allocated from the time evolution of GO surface functionalities.

186x244mm (300 x 300 DPI)

RSC Advances Accepted Manuscript

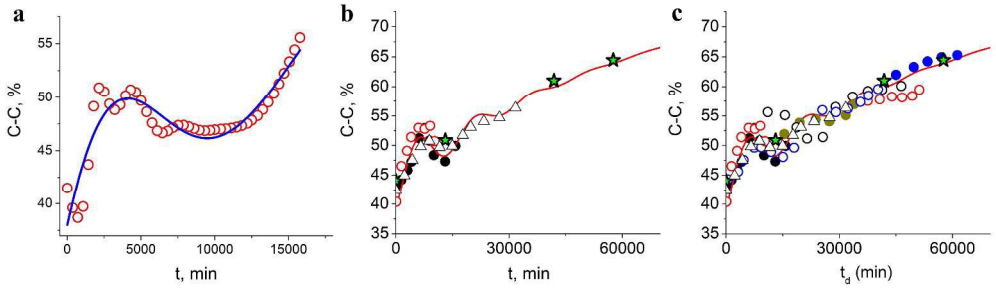

Figure 6. Dependence of C-C concentration on time. (a) Experimental results (red circles) and fitting using the "reactive edges" model (blue curve) of single measurement. (b) Comparison of experimental results started right after GO deposition (symbols), results obtained by S. Kim and co-authors in Ref. 18 (green stars), and the fitting based on the "reactive edges" model (red curve). (c) Comparison of all experimental data in the present work normalized on time elapsed from the deposition procedure (symbols), results obtained by S. Kim and co-authors in Ref. 18 (green stars), and the fitting based on the "reactive edges" model (red curve).

646x186mm (300 x 300 DPI)

RSC Advances Accepted Manuscript